Synthesis and Characterization of Halogenated Derivatives of the Ionophore A23187: Enhanced Calcium Ion Transport Specificity by the 4-Bromo Derivative†

Manuel Debono, R. M. Molloy, D. E. Dorman, J. W. Paschal, Donner F. Babcock, Charles M. Deber, and Douglas R. Pfeiffer*

ABSTRACT: A series of halogenated derivatives of the divalent cation ionophore A23187, 5-(methylamino)-2-[[3,9,11-trimethyl-8-[1-methyl-2-oxo-2-(1*H*-pyrrol-2-yl)ethyl]-1,7-dioxaspiro[5.5]undec-2-yl]methyl]-4-benzoxazolecarboxylic acid, was prepared. Selective bromination or chlorination of the benzoxazole moiety and bromination or iodination of the pyrrole ring system were achieved. Dibromo, diiodo, and tetrabromo derivatives were also prepared and characterized chemically. Examination of ^1H and ^{13}C NMR and of the ultraviolet absorbance spectral properties indicated that the major structural features of A23187–cation complexes are retained in complexes with several of the new compounds. The divalent cation binding properties of 4-bromo-A23187 were investigated by the two-phase extraction technique, and its transport properties were examined in some detail. Affinities of 4-bromo-A23187 for both Ca^{2+} and Mg^{2+} are about 4-fold greater than those of A23187. However, in isolated mitochondria and in intact bovine spermatozoa, the apparent relative transport selectivity of the new ionophore for Ca^{2+} over Mg^{2+} was greater than that observed with A23187. In these systems, cation transport selectivity was dependent upon ionophore dosage. Turnover numbers for Mg^{2+} transport derived from measurement of the initial rates of Mg^{2+} release from mitochondria approached zero at low doses of 4-bromo-A23187. In contrast, turnover numbers for Ca^{2+} transport calculated from steady-state rates of Ca^{2+} transport are insensitive to ionophore concentration and are approximately 50% of those previously observed for A23187. Study of competitive cation transport in sperm suspensions incubated with various extracellular concentrations of Mg^{2+} and Ca^{2+} indicated that cation transport discrimination is also highest at low ionophore dosages. In both systems, at low ionophore concentrations least likely to have undesirable additional actions on biological systems, 4-bromo-A23187 possesses apparent transport selectivity for Ca^{2+} over Mg^{2+} that is approximately 10-fold greater than that exhibited by A23187.

A23187 was the first ionophore shown to transport divalent cations with high selectivity over monovalent cations (Reed & Lardy, 1972). This property has made the ionophore a valuable tool for examination of the regulatory role of divalent cations, particularly Ca^{2+}, in biological systems. Studies employing A23187 have been important in revealing the ubiquitous role of Ca^{2+} as an intracellular regulatory mediator and have contributed to our understanding of the involvement of Ca^{2+} in the control of contraction, secretion, and processes associated with cell division and with other complex biological phenomena [for reviews, see Rasmussen & Goodman (1977) and Kretsinger (1979)]. The use of A23187 as a research tool has also provided insight into the interaction of cellular components that are responsible for regulation of intracellular concentrations and distributions of Ca^{2+} (Ferreira & Lew, 1976; Babcock et al., 1976, 1978, 1979).

Continued progress in these arease as well as in the application of ionophores as pharmacological agents will be dependent in part on the availability of new compounds with known and varied transport properties. Some diversity in the agents available is provided by the discovery of new compounds. At present, 11 naturally occurring ionophores with significant activity for the transport of divalent cations have been identified [for a review, see Taylor et al. (1982)]. Other sources include chemical synthesis of new ionophores [e.g., see Deber et al. (1980)] and chemical modification of known compounds [e.g., see Westley et al. (1973)]. These sources have the potential of providing homologous series of compounds where the structural variations between members are systematic. This approach is expected to have the best chance of providing sets of ionophores whose properties vary as smooth gradations, and where the relationship between structure and function can be understood in the greatest detail.

The present report describes a useful strategy for the selective halogenation of the aromatic substituents of A23187. A series of halogenated derivatives has been prepared, and the transport properties of one of the new compounds have been investigated. The results indicate that compared to the parent compound, 4-bromo-A23187 possesses substantially enhanced transport discrimination between Ca^{2+} and Mg^{2+}.

Experimental Procedures

General Methods. Chromatography of the free acid forms of A23187 and its derivatives on silica gel resulted in severe streaking. Treatment of the silica gel with citric acid alleviated this difficulty, suggesting that it was caused by contaminating cations. Silica gel (Woelm, grade I, 70–150 mesh, 500 g) was suspended in ethanol (2 L) containing citric acid (70 g) and stirred 15 min at room temperature. The supernatant was decanted and the slurry washed twice with toluene and then with benzene (2 L each) and finally dried in vacuo. Separations were routinely achieved upon 50–500-g columns eluted with $CHCl_3$ or benzene. Thin-layer chromatography was performed on silica gel plates sprayed with citric acid and development in a $CHCl_3/CH_3OH$ (95:5 v/v) solvent system.

Starting Materials. A23187 [5-(methylamino)-2-[[3,9,11-trimethyl-8-[1-methyl-2-oxo-2-(1*H*-pyrrol-2-yl)-

† From the Lilly Research Laboratories, Indianapolis, Indiana 46285 (M.D., R.M.M., D.E.D., and J.W.P.); the Institute for Enzyme Research, University of Wisconsin, Madison, Wisconsin 53706 (D.F.B.); the Department of Biochemistry, University of Toronto, Toronto M5S 1A8, and Research Institute, Hospital for Sick Children, Toronto, ON M5G 1X8, Canada (C.M.D.); and the Hormel Institute, University of Minnesota, Austin, Minnesota 55912 (D.R.P.). *Received April 14, 1981.* This work was supported by Grants AM 10334, AM 26277, GM 24701, and HL 08214 from the National Institutes of Health, by Grant MRC 5810 from the Medical Research Council of Canada, by the Eli Lilly Company, and by the Hormel Foundation.

0006-2960/81/0420-6865$01.25/0

ethyl]-1,7-dioxaspiro[5.5]undec-2-yl]methyl]-4-benzoxazolecarboxylic acid] was obtained from fermentation filtrates as the mixed complex with Mg^{2+} and Ca^{2+} (Gale et al., 1976) and was converted to the free acid, **1**, by washing solutions of the complexes in organic solvents with dilute aqueous HCl. The Mg^{2+} complex was subsequently formed by further washing the organic phase with aqueous $MgCl_2$ (Deber & Pfeiffer, 1976). Succinimide, *N*-bromosuccinimide, *N*-chlorosuccinimide, *N*-iodosuccinimide, and pyridinium bromide perbromide were from Aldrich. Iodine monochloride and 1,3-*N*,*N*-dichloro-5,5-dimethylhydantoin were obtained from Fisher and Bromine Products Producers, respectively. The other reagents and solvents are also available from commercial sources and were reagent or spectral grade, respectively.

Spectral Characterization. Optical rotation, optical absorbance, and fluorescence spectra were determined with CH_3OH solutions of the free acid and Mg^{2+} complexes of A23187 and its derivatives. ^1H NMR spectra of the derivatives (10–20 mM in $CDCl_3$) were examined in the aromatic region (6–8 ppm from tetramethylsilane) at 100 MHz. ^{13}C NMR spectra were measured at 25.2 MHz on a JEOL PFT-100 spectrophotometer in $CDCl_3$ solutions. High-resolution mass spectra of the free acid forms of the compounds were obtained with a Varian MAT 731 mass spectrometer.

Reactions and Product Characterization. Mg^{2+} Complex of 4-Bromo-A23187 (**2**). The Mg^{2+} complex of A23187 (1.07 g, 10 mmol) in anhydrous CCl_4 (100 mL) was stirred rapidly with additions of succinimide (0.4 g, 4 mmol) and then of *N*-bromosuccinimide (0.72 g, 4 mmol). After 4–5 h in the dark at room temperature, the yellow reaction mixture was filtered, and solids were washed thoroughly with CCl_4. The combined filtrate and washings were diluted with $CHCl_3$ (300 mL) and washed twice with 2% (w/v) Na_2SO_3 and 3 additional times with H_2O. The organic phase was dried overnight over Na_2SO_4. After solvents were removed in vacuo, the product (1.13 g, 92% yield) was obtained from the foamy residue by crystallization from CH_3OH and was characterized as follows: mp 316–319 °C; $[\alpha]^{25}_D$ +287° (*c* 0.188); mass spectrum, *m/e* 1224 (^{79}Br). Anal. Calcd for $C_{58}H_{70}BrN_6O_{12}\cdot Mg$: C, 56.76; H, 5.74; N, 6.84; Br, 13.02. Found: C, 56.47; H, 5.93; N, 6.78; Br, 14.48.

Free Acid of 4-Bromo-A23187 (**2**). The Mg^{2+} complex of 4-bromo-A23187 (0.86 g, 0.7 mmol) was dissolved in methylene chloride (0.4 L), washed twice with 0.1 N HCl and once with H_2O, and dried over Na_2SO_4. Solvents were removed in vacuo, and the product (0.81 g, 96% yield) was obtained as a yellow foamy residue that was characterized as follows; $[\alpha]^{25}_D$ +26.9° (*c* 3.3). Anal. Calcd for $C_{29}H_{36}BrN_3O_6$: C, 57.81; H, 6.02; N, 6.97; Br, 13.26. Found: C, 57.55; H, 5.77; N, 6.77; Br, 13.52.

Free Acid of 23-Bromo-A23187 (**3**). To the Mg^{2+} complex of A23187 (0.54 g, 0.4 mmol) in glacial acetic acid (30 mL) was added 1 N HCl (1 mL) followed by pyridinium bromide perbromide (0.33 g, 1.0 mmol). The mixture was stirred 30 min at room temperature and then added to an ice–water slurry (100 mL). After 2 h at 5 °C, the precipitate was collected, washed thoroughly with H_2O, and dissolved in $CHCl_3$ (200 mL). This solution was washed twice with 5% (w/v) Na_2SO_3 followed by three additional washings with H_2O. The residue obtained after removal of solvents (0.65 g of pale yellow foam) was applied to a column of citric acid impregnated silica gel (100 g). Elution with benzene and removal of solvent gave a nearly colorless foam (0.43 g) that was dissolved in $CHCl_3$ (100 mL), washed twice with H_2O, and allowed to stand overnight. The recovered crystalline product (0.25 g, 42% yield) was characterized as follows: mp 180–183 °C; $[\alpha]^{25}_D$ +30.4° (*c* 0.30). Anal. Calcd for $C_{29}H_{36}BrN_3O_6$: C, 57.81; H, 6.02; N, 6.97; Br, 13.26. Found: C, 57.87; H, 6.03; N, 6.68; Br, 12.90.

Free Acid of 23,24-Dibromo-A23187 (**4**). The product was prepared as described for **3** except that the reaction mixtures were doubled in size and a 4-fold molar excess of pyridinium bromide perbromide was employed. After solvent removal, the foamy yellow residue (1.26 g, 93% yield) was characterized as follows; [a]$^{25}_D$ −120.2° (*c* 2). Anal. Calcd for $C_{29}H_{35}Br_2N_3O_6$: C, 51.12; H, 5.18; N, 6.17; Br, 23.45. Found: C, 51.39; H, 5.31; N, 6.23; Br, 23.2.

Mg^{2+} Complex of 23,24-Dibromo-A23187 (**4**). Magnesium acetate (1.5 g, 10 mmol) in H_2O (15 mL) was added to a solution of the free acid of **4** (150 mg, 0.22 mmol) in dioxane (20 mL). After the mixture was stirred overnight at room temperature, the volume was reduced to 18 mL in vacuo. Water (40 mL) was added and the precipitate collected, dissolved in $CHCl_3$, and applied to a silica gel column (200 g). The product (62 mg, 40% yield) was eluted with and crystallized from $CHCl_3$ and characterized as follows: mp 322–325 °C; $[\alpha]^{25}_D$ +101.3° (*c* 0.31). Anal. Calcd for $C_{58}H_{68}Br_4N_6O_{12}\cdot Mg$: C, 50.28; H, 4.94; N, 6.06; Br, 23.07. Found: C, 50.09; H, 4.95; N, 5.84; Br, 23.29.

Free Acids of 4,23-Dibromo-A23187 (**5**) *and 4,22,23,24-Tetrabromo-A23187* (**6**). To the Mg^{2+} complex of A23187 (107 mg, 0.1 mmol) dissolved in CCl_4 (10 mL) was added succinimide (80 mg, 0.8 mmol) and then *N*-bromosuccinimide (144 mg, 0.8 mmol). After being stirred for 54 h in the dark at room temperature, the yellow reaction mixture was cooled to 5 °C and filtered, and the solids were washed thoroughly with CCl_4. The combined filtrate and washings were concentrated to dryness, and the resulting residue was redissolved in $CHCl_3$. This solution was washed sequentially with 2% (w/v) Na_2SO_3 and then H_2O and dried over Na_2SO_4 overnight at 5 °C in the dark. A yellow foamy residue (128 mg) was obtained after solvent removal. Application of this material to a column of citrate-impregnated silica gel (50 g) followed by elution with $CHCl_3$ gave pure **6** (27 mg, 6% yield) that was characterized as follows; $[\alpha]^{25}_D$ +35.6° (*c* 2). Further elution with $CHCl_3$ gave pure **5** isolated as a foamy residue (32 mg, 24% yield) that was characterized as follows; $[\alpha]^{25}_D$ +47.7° (*c* 2). Anal. Calcd for $C_{29}H_{35}Br_2N_3O_6$: C, 51.12; H, 5.18; N, 6.17; Br, 23.45. Found: C, 51.42; H, 5.32; N, 5.93; Br, 23.40.

Mg^{2+} Complex of 4-Chloro-A23187 (**7**). To the Mg^{2+} complex of A23187 (5.34 g, 5.0 mmol) in CCl_4 (1 L) was added pyridine (anhydrous, 15 mL) and then 1,3-*N*,*N*-dichloro-5,5-dimethylhydantoin (1.97 g, 10 mmol). The mixture was heated to 60 °C for 4 h in the dark and then cooled and concentrated in vacuo to near dryness. The yellow syrup was diluted with $CHCl_3$ (1 L) and washed twice with 2% (w/v) Na_2SO_3 and then with H_2O. Solvents were removed in vacuo after drying overnight over Na_2SO_4. The product (4.06 g, 71% yield) was obtained by crystallization of the foamy residue from CH_3OH and characterized as follows: mp 313–317 °C; $[\alpha]^{25}_D$ +331.7° (*c* 0.97). Anal. Calcd for $C_{58}H_{70}N_6O_{12}Cl_2\cdot Mg$: C, 61.18; H, 6.20; N, 7.38; Cl, 6.22. Found: C, 61.13; H, 6.15; N, 7.17; Cl, 6.47.

Free Acid of 4-Chloro-A23187 (**7**). The Mg^{2+} complex of **5** (100 mg, 0.09 mmol) dissolved in $CHCl_3$ (50 mL) was washed twice with 0.1 N HCl and then twice with H_2O. The organic phase was dried over Na_2SO_4, and solvents were removed to leave the product (93 mg, 95% yield) as a foamy residue that was characterized as follows; $[\alpha]^{25}_D$ +30.4° (*c*

4.0). Anal. Calcd for $C_{29}H_{36}N_3O_6Cl$: C, 62.41; H, 6.50; N, 7.53; Cl, 6.35. Found: C, 62.18; H, 6.32; N, 7.23; Cl, 6.61.

Free Acid of 23-Iodo-A23187 (**8**). To the Mg^{2+} complex of A23187 (534 mg, 0.5 mmol) in glacial acetic acid (20 mL) containing 0.05 M HCl was added iodine monochloride (162 mg, 1.0 mmol). The deep violet mixture was stirred 30 min at room temperature, poured onto an ice–water slurry (300 mL), and then extracted 3 times with $CHCl_3$. The combined extracts were washed with H_2O, 2% (w/v) Na_2SO_3, H_2O, 0.1 N HCl, and again with H_2O. The organic layer was dried over Na_2SO_4 and concentrated in vacuo. The yellow foamy residue (612 mg) was applied to a citrate-impregnated silica gel column (350 g) and eluted with $CHCl_3$. The collected eluate was concentrated to dryness, and the residue (556 mg) was redissolved in $CHCl_3$ and dried over Na_2SO_4. The product (287 mg, 44% yield) was recrystallized from diethyl ether/petroleum ether (1:4) and characterized as follows: mp 186–188 °C; $[\alpha]^{25}_D$ +9.9° (*c* 0.021). Anal. Calcd for $C_{29}H_{36}N_3O_6I$: C, 53.63; H, 5.59; N, 6.47; I, 19.54. Found: C, 53.76; H, 5.66; N, 6.24; I, 19.57.

Free Acid of 23,24-Diiodo-A23187 (**9**). To the Mg^{2+} complex of A23187 (0.53 g, 0.5 mmol) in glacial acetic acid (20 mL) containing 0.05 M HCl was added ICl (325 mg, 2.0 mmol). The reaction was treated as for the preparation of **6**. The residues before and after chromatography consisted of 642 and 280 mg, respectively. Concentration of the washed eluate gave the product (178 mg, 23% yield) as a foam that was characterized as follows: $[\alpha]^{25}_D$ +22.9° (*c* 2.0). Anal. Calcd for $C_{29}H_{35}N_{35}N_3O_6I$: C, 44.97; H, 4.55; N, 5.42; I, 32.73. Found: C, 45.17; H, 4.60; N, 5.18; I, 33.08.

Cation Binding and Transport Methods. Two-phase extraction cation binding constants were determined as described by Pfeiffer & Lardy (1976). Rat liver mitochondria were prepared by a standard procedure (Pfeiffer et al., 1976). For determination of the ionophore's turnover number for Ca^{2+} transport, the rate of succinate oxidation, activated by ionophore-induced cycling of Ca^{2+}, was investigated as a function of the amount of ionophore present. The maximal slope of this plot, multiplied by 4 (to account for the Ca^{2+}/O ratio with succinate as substrate), was taken as the Ca^{2+} turnover number (Pfeiffer et al., 1976; Kauffman et al., 1980). Oxygen consumption was determined with a Gilson oxygraph utilizing a Clark-type oxygen electrode. Turnover numbers for Mg^{2+} transport in mitochondria were calculated from rates of depletion by using eriochrome blue SE as a Mg^{2+}-indicating dye (Scarpa, 1974). Mitochondria were incubated under conditions similar to those used to determine Ca^{2+} tunover in media containing the dye at 100 μM. Following addition of the ionophore at appropriate levels, the change in the difference absorbance at 575 vs. 540 nm as a function of time was used to calculate the rate of Mg^{2+} efflux.

The effect of extracellular Mg^{2+} concentration on Ca^{2+} transport induced by ionophores was investigated in a cellular system. Bovine epididymal spermatozoa were prepared and incubated in vitro in the presence of the metallochromic indicator dye murexide as described previously (Babcock et al., 1976). Ca^{2+} uptake and release by the cells were monitored at the wavelength pair 540 vs. 507 nm. All difference absorbance measurements were made with the Aminco DW2 dual-wavelength spectrophotometer.

Results

Synthesis and Chemical Properties of A23187 Derivatives. Preliminary attempts to prepare halogenated derivatives of the free acid form of A23187 (**1**) yielded several products in low yield (Figure 1). A more controlled reaction was achieved

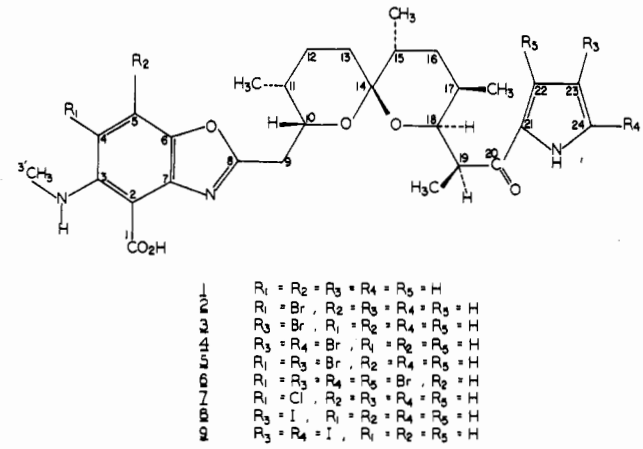

FIGURE 1: Numbering system and structures of A23187 and the halogenated derivatives. The structure of the parent compound was determined by Chaney et al. (1974) and is projected as suggested by Westley (1976). The designations **1**–**9** give the identity of the five atoms (R groups) which vary in the derivatives.

by treatment of the Mg^{2+} complex of **1** with *N*-bromosuccinimide. ^1H NMR spectra of the predominant product **2** showed only a 7.80-ppm signal integrating to two protons in the benzoxazole proton region, approximately 0.5 ppm downfield from the H_5 resonance of the parent compound (Deber & Pfeiffer, 1976). Assignment to H_5 was confirmed by the absence of the nuclear Overhauser effect that is observed with the parent compound upon irradiation of the carbon 3′ protons (2.98 ppm) (Chaney et al., 1974). In the pyrrole proton region of the spectrum of **2**, the presence of 6.25-, 7.00-, and 7.37-ppm signals integrating to six protons indicated that the site of bromination was restricted to the benzoxazole ring system. The mass spectral fragmentation pattern of the free acid form of **2** showed prominent features identical with those found for **1** by Chaney et al. (1974). The presence of *m/e* 94 (C_5H_4NO) and *m/e* 284 ($C_{10}H_8BrN_2O_3$) fragments corresponding to unmodified pyrrole and monobromobenzoxazole portions of **2**, respectively, confirmed the exclusive nature of the bromination site at carbon 4.

Reaction of the Mg^{2+} complex of **1** with *N*-chlorosuccinimide was not as successful. The reagent was both less reactive and less selective. However, treatment with 1,3-*N*,*N*-dichloro-5,5-dimethylhydantoin in pyridine produced selective substitution of Cl on the benzoxazole ring. Examination of the ^1H NMR spectrum of the predominant reaction product **7** by the same techniques described for **2** confirmed the site of substitution at carbon 4.

Reaction of the Mg^{2+} complex of **1** with *N*-iodosuccinimide or with ICl gave a mixture of products. The best results were obtained by using ICl in acidified acetic acid. With equimolar ratios of **1** and ICl, a monoiodo derivative (**8**) was obtained as the free acid after silica gel chromatography. Analysis by ^1H and ^{13}C NMR indicated that substitution was confined to the pyrrole ring (see Table I for the chemical shifts of aromatic group carbon atoms in A23187 and selected derivatives) and observed coupling of the multiplet pyrrole protons is consistent with localization at carbon 23.

When the molar ratio of ICl was doubled, a diiodo derivative (**9**) was obtained. Its ^1H NMR spectrum contained benzoxazole proton signals at 6.98 and 7.08 ppm but only a single broad pyrrole proton doublet resonance (6.94 ppm, J = 3.5 Hz). The mass spectrum of **9** includes the diagnostic fragments *m/e* 346 (diiodoketopyrrole) and *m/e* 206 (benzoxazole fragment), confirming that substitution is confined to the two positions in the pyrrole ring. ^{13}C NMR spectra of **9** contain two signals, 86.2 and 76.7 ppm, that are shifted upfield by 38.3

Table I: Chemical Shifts of the Aromatic Carbon Atoms in A23187 and Selected Derivatives[a]

carbon no.	A23187 (1)	4-bromo-A23187 (2)	4-chloro-A23187 (7)	23-iodo-A23187 (8)	23,24-diiodo-A23187 (9)
C_1	168.2	167.2	167.1		
C_2	97.9	106.5	98.5		
C_3	150.8	150.7	149.7		
$C_{3'}$	30.0	36.5	34.9		
C_4	108.4	110.6	121.5		
C_5	116.4	121.4	118.1		
C_6	140.8	143.3	142.3		
C_7	141.6	140.9	140.3		
C_{20}	193.6			193.3	192.0
C_{21}	133.1			134.4	138.5
C_{22}	116.4			122.3	123.5
C_{23}	110.1			61.5	76.7
C_{24}	124.5			129.2	86.2

[a] ^{13}C NMR spectra were obtained as described under Experimental Procedures. Chemical shifts are given in parts per million vs. an internal tetramethylsilane standard. The carbon atom numbering system and derivative structures are depicted in Figure 1.

Table II: Chemical Shifts of Hinge Region Atoms in A23187 and Selected Derivatives[a]

atom no.	A23187 (1) (Mg^{2+} complex)	4-bromo-A23187 (2) (Mg^{2+} complex)	4,23-dibromo-A23187 (4) (Mg^{2+} complex)	4-chloro-A23187 (7) (Mg^{2+} complex)
C_{10}	72.8	72.9	72.6	72.9
	(71.6)	(71.7)	(71.5)	(71.7)
C_{18}	68.3	68.4	68.8	67.5
	(74.8)	(74.8)	(75.0)	(74.9)
H_{10}	4.26	4.23	4.17	4.24
	(3.99)	(4.01)	(3.97)	(4.00)
H_{18}	3.69	3.59	3.59	3.61
	(2.69)	(2.73)	(2.75)	(2.75)

[a] ^{13}C and ^1H NMR spectra were obtained as described under Experimental Procedures. Chemical shifts are given in parts per million vs. an internal trimethylsilane standard. For each atom, the value presented without parentheses refers to the free acid form of the compound designated at the top of the column containing the number. The value in parentheses refers to the compound in the Mg^{2+} complex form. The carbon atom numbering system and derivative structures are depicted in Figure 1.

Table III: UV Spectral Absorption Maxima and Extinction Coefficients of A23187 Derivatives and Their Mg^{2+} Complexes

compd	λ (nm), $\epsilon \times 10^{-3}$: free acid	λ (nm), $\epsilon \times 10^{-3}$: Mg^{2+} complex
4-bromo-A23187 (2)	227, 21.0	231, 39.4
	290, 15.6	305, 32.0
	340 (s), 4.0	340 (s), 10.0
23-bromo-A23187 (3)	228, 24.2	229, 54.5
	311, 11.1	310, 26.0
	370, 7.5	371, 16.0
23,24-dibromo-A23187 (4)	226, 28.1	228, 46.1
	278, 13.5	305, 18.0
	298, 16.0	328, 19.2
	377, 8.5	365, 12.0
4,23-dibromo-A23187 (5)	208, 14.1	
	293, 8.4	
4,22,23,24-tetrabromo-A23187 (6)	230, 6.6	
	299 (s), 14.2	
4-chloro-A23187 (7)	226, 19.4	228, 4.5
	289, 14.4	304, 3.4
		340 (s), 10.8
23-iodo-A23187 (8)	226, 26.7	
	253, 13.8	
	299, 11.5	
	375, 7.8	
23,24-diiodo-A23187 (9)	220, 27.2	
	250, 11.0	
	308, 14.3	
	365, 5.5	

[a] Data were obtained in methanol as described under Experimental Procedures. The designation λ refers to the wavelength of maximum absorbance for the absorbing band in question. The symbol (s) following the wavelength designation indicates that the band appeared as a shoulder. $\epsilon \times 10^{-3}$ is the apparent extinction coefficient of the designated absorbing band divided by 10^3. The derivative structures are depicted in Figure 1.

and 30.4 ppm, respectively, from the corresponding carbon 23 and 24 signals of the free acid form of **1**, indicating that these are the sites of substitution.

Selective bromination of the pyrrole ring of **1** was achieved by reaction with an equimolar ratio of pyridinium bromide perbromide in acidified acetic acid. The ^1H NMR spectrum of the product **3** contained nearly unaltered doublet benzoxazole proton signals (6.63, 7.57 ppm; $J = 9.0$ Hz) but only two signals ascribable to pyrrole aromatic protons, 6.89 and 7.04 ppm, that are transformed to doublets by D_2O exchange ($J = 1.5$ Hz). The small coupling between these pyrrole proton resonances indicates a 1,3 relationship and thus substitution at carbon 23.

Reaction of the Mg^{2+} complex of **1** with a 4-fold molar excess of pyridinium bromide perbromide produced the dibromo derivative **4**, whose ^1H NMR spectrum contains both benzoxazole proton signals but only one pyrrole proton resonance (6.91 ppm, s, 1 H) equivalent to the hydrogen 22 resonance of **1**. A nuclear Overhauser effect was obtained upon irradiation of the free acid form of [1] at the hydrogen 19 resonance (3.1–3.2 ppm). A corresponding nuclear Overhauser effect was obtained for **4**, indicating substitution at carbons 23 and 24.

Reaction of the Mg^{2+} complex of **1** with a 4-fold molar excess of *N*-bromosuccinimide gave a mixture of two products that were separated by chromatography on silica gel. The ^1H NMR spectra of the more mobile product (**6**) contained no pyrrole proton signals and a single benzoxazole proton resonance at 7.93 ppm, assigned to the H_4 position. The mass spectrum showed a molecular ion, *m/e* 835 (attributable to $C_{29}H_{33}Br_4N_3O_6$), and peaks at *m/e* 328 (tribromoketopyrrole fragment) and *m/e* 396 (monobromobenzoxazole fragment) that support substitution at positions 4, 22, 23, and 24. ^1H NMR spectra of the second product (**5**) isolated from this reaction contained two pyrrole proton resonances at 6.90 and 7.06 ppm and a single benzoxazole proton signal at 7.93 ppm, thus indicating substitution at sites 4 and 23 in this dibromo derivative.

Comparison of chemical shifts in the ^{13}C NMR spectra of A23187 with those of several halo derivatives indicated that little or no alteration had occurred in the aliphatic spiro ketal region of the compounds (data not shown). Small shifts were observed in the resonances of carbons in the aromatic ring systems that bear the halo substituents in compounds **2**, **7**, **8**, and **9** (Table I). The properties of the critical hinge-region carbons which link the aromatic liganding groups to the spiro ketal moiety and control the molecule's conformation (Deber & Pfeiffer, 1976; Pfeiffer & Deber, 1979) were examined by ^{13}C and ^1H NMR in the free acid and Mg^{2+} complex forms of the parent compound and several derivatives (Table II). The observed resonance shifts indicate that similar reorientations at carbons 10 and 18 occur upon cation complexation with A23187 and with derivatives **2**, **5**, and **7**. The ultraviolet

Table IV: Equilibrium Extraction Constants (K_{ex}) for Cation Complexation by A23187 and 4-Bromo-A23187[a]

compd	stoichiometry (ionophore: cation) Ca^{2+}	stoichiometry (ionophore: cation) Mg^{2+}	K_{ex} Ca^{2+}	K_{ex} Mg^{2+}	$K_{ex}^{Ca^{2+}}/K_{ex}^{Mg^{2+}}$
A23187 (1)	2:1	2:1	3.7×10^{-7}	1.3×10^{-7}	2.8
4-bromo-A23187 (2)	2:1	2:1	1.6×10^{-6}	5.0×10^{-7}	3.2
4-bromo-A23187/A23187			4.3	3.8	

[a] The cation complexes were formed in an aqueous-organic biphasic system. At saturation, the mole ratio of divalent cation to ionophore in the organic phase approached 0.5, indicating a 2:1 ionophore:cation complex stoichiometry. Under these conditions, the complex is formed according to the reaction $2AH_{org} + M^{2+}_{aq} \rightleftharpoons A_2M_{org} + 2H^+_{aq}$, where AH_{org} is the organic phase, M^{2+}_{aq} is divalent metal cation in the aqueous phase, A_2M is the 2:1 ionophore:divalent cation complex in the organic phase, and H^+ hydrogen ion in the aqueous phase. Equilibrium extraction constants (K_{ex}) are then defined by the relationship $K_{ex} = (A_2M)_{org}(H^+)^2_{aq}/[(AH)^2_{org}(M^{2+})_{aq}]$ [see Pfeiffer & Lardy (1976)]. The organic phase (4.0 mL of 70% toluene and 30% butanol) contained the ionophore at 100 μM. The aqueous phase (2.0 mL) contained 50 mM β,β'-dimethylglutaric acid or Tris as buffer and $CaCl_2$ or $MgCl_2$ at 5.0 mM. The position of the equilibrium was varied by altering the aqueous phase pH, and the concentration of A_2M in the organic phase was determined from atomic absorption measurements. These data allow calculation of K_{ex} [see Pfeiffer & Lardy (1976) for further details]. The column Ca^{2+}/Mg^{2+} expresses the relative stabilities of the Ca^{2+} compared to the Mg^{2+} complexes for the ionophore indicated. The row 4-bromo-A23187/A23187 expresses the relative stabilities of the derivative compared to the parent compound for the cation indicated.

absorption spectra (Table III) also suggest similar structures for the complexes of the parent compound and the derivatives **2**, **3**, **4**, and **7**.

Cation Binding and Transport by 4-Bromo-A23187. Structural similarities of the metal ion complexes of **1** and **2** are reflected in the stoichiometry and stability of the Ca^{2+} and Mg^{2+} complexes (Table IV). The new compound extracts either of these cations from a bulk aqueous to a bulk organic phase, forming complexes with the same 2:1 stoichiometry as does A23187. The equilibrium extraction constants demonstrate that the complexes with the new ionophore are approximately 4-fold more stable than those with the parent compound under these conditions. The relative binding discrimination between these two cations has not been appreciably altered. These findings suggest that the effect of bromination on complex stability arises primarily through changes in the protonation constant and changes in the electron densities of the benzoxazole cation liganding atoms. These factors would have equivalent effects on the stability of complexes with chemically similar cations.

Relative complex stabilities are often a major determinant of an ionophore's relative transport efficiency for different cations [for a review, see Taylor et al. (1982)]. Thus, one might predict that the new ionophore would have comparable relative transport efficiencies for Ca^{2+} compared to Mg^{2+}. However, this is not the case. Figure 2 compares the transport efficiency of A23187 and the 4-bromo analogue for Ca^{2+} in mitochondria. Like the parent compound, addition of increasing levels of 4-bromo-A23187 produces a progressive increase in the rate of succinate oxidation. Accelerated respiration was prevented by the Ca^{2+} chelator ethylene glycol bis(β-aminoethyl ether)-*N,N,N'N'*-tetraacetic acid (EGTA) or by the Ca^{2+} transport inhibitor ruthenium red (data not shown). These properties indicate that acclerated respiration

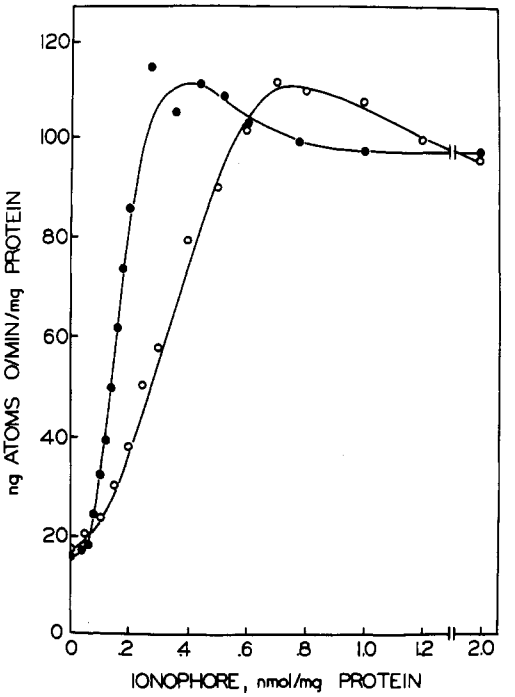

FIGURE 2: Activation of mitochondrial respiration by A23187 and 4-bromo-A23187. Mitochondria were incubated at 2.5 mg of protein/mL, 25 °C, in 0.23 M mannitol, 0.07 M sucrose, 10 mM succinate (Na^+) plus rotenone (0.5 nmol/mg of protein), and triethanolamine (Cl^-), pH 7.4. After being allowed to accumulate 30 nmol/mg of protein of Ca^{2+}, the indicated level of ionophore was added and the rate of oxygen consumption observed (see Experimental Procedures). (●) A23187; (○) 4-bromo-A23187.

is due to an energy-dissipating cyclic flux of Ca^{2+} across the inner mitochondrial membrane established by the new ionophore and endogenous Ca^{2+} uniporter, equivalent to the effects of the parent compound reported previously (Reed & Lardy, 1972; Pfeiffer et al., 1976). Thus, in the region where the relationship between ionophore level and rate of oxidation is linear, the ionophore's turnover number for Ca^{2+} transport can be estimated from the transport rates obtained by multiplying the slope of the line by four to account for the Ca^{2+}/O ratio of this substrate (Pfeiffer et al., 1976). From the data in Figure 2, the turnover numbers are 44 and 22 s^{-1} for A23187 and the 4-bromo derivative, respectively. Thus, whereas the Ca^{2+} complex of the new ionophore is 4-fold more stable than that of the parent compound, its turnover number is smaller by a factor of two.

The turnovers for Mg^{2+} transport were obtained from experiments similar to those shown in Figure 2, except that the mitochondria were not loaded with Ca^{2+}, and EGTA was included in the incubation medium to prevent cycling of endogenous Ca^{2+}. Thus, turnover numbers were obtained under conditions where all the added ionophore was available for Mg^{2+} transport. Figure 3A shows that in contrast to the results obtained for Ca^{2+} transport, the rate of Mg^{2+} transport was not a linear function of the ionophore level for either compound. Turnover numbers calculated from these data (Figure 3B) show that at the lowest level of A23187 tested the value obtained is approximately 30-fold less than that for Ca^{2+} transport as obtained from Figure 2. This finding is of interest in itself in that the relative affinity of A23187 for these two cations differs by only 2–3-fold (see Table IV). As the level of the ionophore increases, the turnover number for Mg^{2+} transport progressively rises and thus tends to converge with the constant value for Ca^{2+} transport.

The new ionophore displays qualitatively the same behavior although quantitatively there are important differences. At

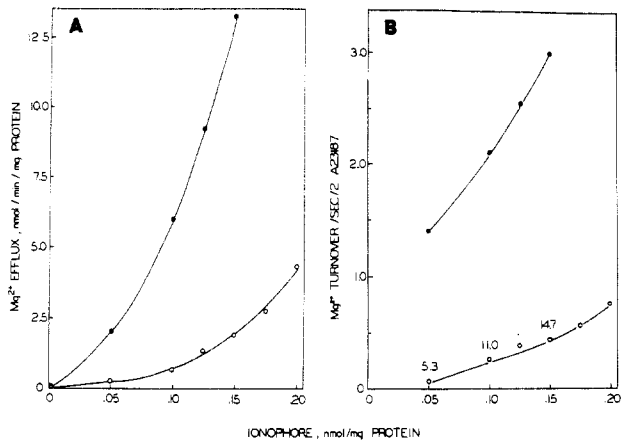

FIGURE 3: The effect of ionophore level on rates and turnover numbers for Mg^{2+} transport in mitochondria. Mitochondria were incubated as described in the legend to Figure 2 except that the buffer was 20 mM Hepes (Na^+), the addition of $CaCl_2$ was omitted, and 100 μM each of EGTA and eriochrome blue SE was present in the media. After a 2-min period of equilibration, the indicated level of ionophore was added an the rate of Mg^{2+} depletion observed (see Experimental Procedures). Turnover numbers were calculated from these data. Efflux rates and turnover numbers are shown in panels A and B, respectively. (●) A23187; (○) 4-bromo-A23187.

the lowest level tested, 4-bromo-A23187 was almost inactive for Mg^{2+} transport. The turnover number again increased progressively as the amount was increased. At the lowest level tested, 4-bromo-A23187 is only 5.3% as active as the parent compound. From these data and the Ca^{2+} turnover number obtained from Figure 2, the relative transport efficiency of 4-bromo-A23187 for Ca^{2+} is approximately 300 times the value for Mg^{2+}, or a 10-fold improvement over the relative transport efficiency obtained with A23187. The data further show that this differential decreases at higher levels of the compounds.

Previous studies of the action of A23187 at the cellular level revealed a bimodal effect of the ionophore upon Ca^{2+} movements in spermatozoa (Babcock et al., 1976, 1978). Bovine sperm accumulate substantial amounts of exogenously added Ca^{2+} during incubation in vitro. Addition of a low level of A23187 induces release of the accumulated cation, and a second larger addition of ionophore induces reuptake of Ca^{2+}. The initial uptake represents energy-dependent mitochondrial accumulation. The first addition of ionophore releases Ca^{2+} to the cytoplasmic space with subsequent expulsion from the cells by a vectorial pump located in the plasma membrane. Larger ionophore additions exceed the transport capacity of this outward-directed pump and allow equilibration of extracellular and cytosolic Ca^{2+} concentrations. Thus, small additions of A23187 to spermatozoa and other cellular systems (Borle & Studer, 1978; Chen et al., 1978; Chandler & Williams, 1978; Babcock et al., 1979) resulted in a preferential action of the ionophore on Ca^{2+} distributions across the membranes of mitochondria in situ. Figure 4 compares the influence of extracellular Mg^{2+} concentrations upon ionophore-induced release and uptake of Ca^{2+}. Extracellular Mg^{2+} inhibits both the rate and the extent of Ca^{2+} uptake induced by A23187 (Figure 4A,C), as a result, in part, of the competition between the Mg^{2+} and Ca^{2+} cations for complex formation with ionophore present at the external surface of the plasma membrane. Release of accumulated Ca^{2+} stores by A23187 is affected much less, presumably because the extracellular cation concentrations do not appreciably alter the environment of the ionophore present at the mitochondrial membrane interface.

The 4-bromo derivative (**2**) also has a bimodal action on sperm Ca^{2+} fluxes (Figure 4B,C). Whereas the observed rate of release of mitochondrial Ca^{2+} is slower, the reuptake of Ca^{2+} is faster than that induced by equivalent doses of A23187. Possible explanations include alterations in the partitioning of the derivative into cellular membranes or of secondary effects upon ion pumps.

Most importantly, comparison of panels A and B of Figure 4 demonstrates that Ca^{2+} uptake induced by **2** is substantially more resistant to inhibition by extracellular Mg^{2+} than is uptake induced by A23187. Figure 4C summarizes these

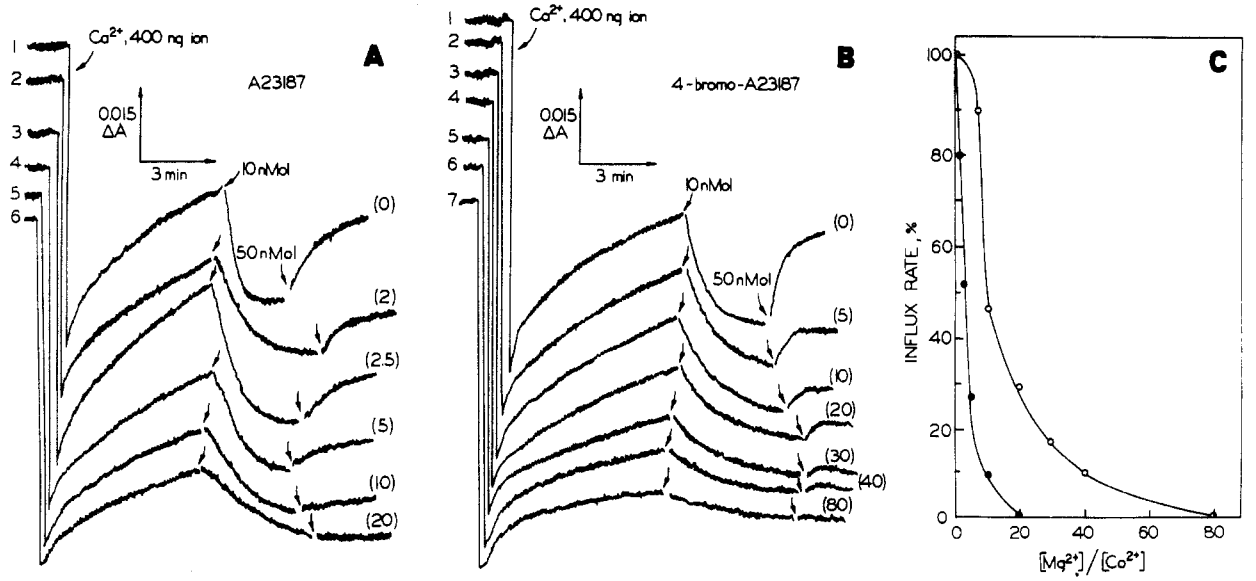

FIGURE 4: Effect of Mg^{2+} concentration on Ca^{2+} transport in spermatozoa induced by A23187 and 4-bromo-A23187. (A) Washed spermatozoa (4.5×10^8 cells) were suspended in 0.25 M mannitol, 0.07 M sucrose, 5.0 mM fructose, 10 mM morpholinopropanesulfonate (Na^+), 1.0 mM phosphate (Na^+), pH 7.4, 0.10 mM murexide, and 0–8 μmol of $MgCl_2$ in a total volume of 2.5 mL. Addition of $CaCl_2$ (400 nmol) was made as shown in tracings 1–5 to produce the molar ratios (Mg^{2+}/Ca^{2+}) indicated parenthetically. An increase in the murexide difference absorbance indicates a decrease in the extracellular Ca^{2+} concentration. Release of accumulated Ca^{2+} was initiated by addition of 10 nmol of A23187 and reuptake by addition of 50 nmol of A23187. (B) Conditions were as described above except that 0–32 μmol of Mg^{2+} was present and 4-bromo-A23187 replaced A23187. (C) The Ca^{2+} influx rate following addition of the second aliquot of ionophore A23187 (●) or 4-bromo-A23187 (○) is shown as a function of the ratio of initial extracellular Mg^{2+} and Ca^{2+} concentrations. Data are normalized to the rate observed in the absence of added Mg^{2+}.

Table V: Effect of Ionophore Concentration on Inhibition of Ca^{2+} Uptake by Mg^{2+}[a]

ionophore concn (nmol/mg of protein)	% inhibition by Mg^{2+} of Ca^{2+} uptake induced by	
	A23187	4-bromo-A23187
1.0		79
1.5		75
1.9	97	
2.9	85	70
5.7	51	

[a] Experiments were performed as described in Figure 4 except that additions of 20 and 100 nmol of 4-bromo-A23187 were employed with cell suspensions containing (4–12) × 10^8 sperm and either 0 or 4 μmol of $MgCl_2$. Additions of 10 and 50 μmol of A23187 were made to cell suspensions containing (4–12) × 10^8 sperm and 0 or 1 μmol of $MgCl_2$. Apparent rates of Ca^{2+} uptake in the absence of Mg^{2+} were 3.1, 9.1, and 15.4 nmol (10^8 cells)$^{-1}$ min^{-1} and 3.5, 13.3, and 25.6 nmol (10^8 cells)$^{-1}$ min^{-1}, respectively, for the indicated additions of A23187 or 4-bromo-A23187, respectively.

experiments and indicates that under the described conditions 50% inhibition was observed at extracellular Mg^2/Ca^{2+} molar ratios of 2.5 and 10 for ionophores **1** and **2**, respectively. With the assumption that inhibition of Ca^{2+} uptake by Mg^{2+} results from competition between the cations for transport by the ionophore, transport selectivity for Ca^{2+} by 4-bromo-A23187 was approximatley 4-fold that exhibited by A23187 under these conditions. In experiments similar to those in Figure 4, it was found that at lower ionophore concentrations 4-bromo-A23187 demonstrated a 10-fold increase in relative transport selectivity (data not shown) and that the inhibitory action of extracellular Mg^{2+} upon Ca^{2+} transport was relieved by higher doses of the ionophore (Table V). In this respect, the selectivity of transport induced by A23187 shows a greater dependence upon ionophore concentration than that induced by 4-bromo-A23187. As with the experiments conducted with isolated mitochondria (Figure 3), an explanation for these dose-dependent effects upon relative transport efficiencies is not apparent.

Discussion

Attempts to halogenate the free acid form of A23187 or its methyl ester produced mixtures of products with one or more substitutions in the aromatic ring systems. The location of the substitution sites was consistent with the electronic effects of the other substituents on the benzoxazole and pyrrole nuclei. Upon reaction of *N*-halosuccinimides with the metal ion complex form of A23187, substitution proceeded more readily, and a more selective halogenation was achieved. This specificity may be the result of both steric constraints imposed by complex formation and electron withdrawal by the divalent cation with resulting deactivation of the aromatic rings to attack at particular positions. Reaction of A23187 in the free acid form with pyridinium bromide perbromide under acidic conditions produced pyrrole substitution exclusively. Specificity in this case may be conferred by protonation of the $N\text{-}CH_3$ group with resultant deactivation of the benzoxazole ring.

The stoichiometry of the neutral Ca^{2+} and Mg^{2+} complexes with 4-bromo-A23187 was found to be the same as that with A23187. Examination of ^1H and ^{13}C NMR and ultraviolet spectral properties indicates that the overall conformation of the free acid and metal ion complex forms of several of the derivatives closely resembles those of the parent compound. These results are consistent with confinement of the substitution sites to locations on the aromatic nuclei that are oriented to the exterior of the metal ion complex structures deduced previously from X-ray crystallographic (Chaney et al., 1974; Smith & Duax, 1976) and NMR (Deber & Pfeiffer, 1976; Anteunis, 1977; Pfeiffer & Deber, 1979) studies.

A23187 has proven an extremely useful tool in the study of Ca^{2+} as a regulatory mediator. However, in complex biological systems, the ionophore has a number of actions in addition to the discharge of Ca^{2+} gradients that exist across the membranes of cells and their internal organelles [e.g., see Klausner et al. (1979), Dordick et al. (1980), and Ben-Hayyim & Krause (1980)]. Among such actions, ionophore-induced transport of Mg^{2+} has been useful in studies of chloroplast function [see Sokolove (1979) and Ben-Hayyim & Krause (1980) and references cited therein] but has been a complicating influence in most other studies employing A23187. Characterization of 4-bromo-A23187 described in the present studies indicates that this new ionophore possesses enhanced selectivity between Ca^{2+} and Mg^{2+} for transport across the membranes of isolated mitochondria and across the surface membranes of sperm. At the low ionophore concentrations least likely to produce other undesirable actions, it is estimated that the increase in selectivity for 4-bromo-A23187 compared to A23187 is greater than 10 times in both sperm and mitochondrial systems. Preliminary experiments (D. F. Babcock, unpublished results) indicate that in the absence of extracellular Mg^{2+} the magnitude of transmembrane proton gradients is the major determinant of the extent of Ca^{2+} fluxes induced by ionophore treatment of bovine sperm. This finding indicates that the reduction of the extent of Ca^{2+} influx in the presence of extracellular Mg^{2+} (Figure 4) is a result of Mg^{2+} uptake and that the accompanying reduction in the rate of Ca^{2+} uptake arises from competitive transport, rather than from other factors peculiar to sperm. It is expected, therefore, that 4-bromo-A23187 will also exhibit enhanced transport selectivity for Ca^{2+} in other cellular systems.

Examination of complex stabilities in bulk phase transport studies does not provide an explanation for the altered transport specificity of 4-bromo-A23187 in isolated mitochondria or bovine sperm observed here. These systems are inherently complex, and further work with model transport systems will be required to elucidate the mechanisms that underlie this alteration. Factors that may be involved in altering transport selectivity include changes in membrane–aqueous phase partition coefficients or ionophore–membrane interactions, changes in the complexation–decomplexation kinetic constants, altered diffusion constants for the transmembrane movement of the ionophore, or others.

As a final point, it was noted that the fluorescence of the benzoxazole chromophore is lost upon bromination at position 4 (data not shown). This change in spectral properties should be useful in biochemical applications where ionophores are employed in conjunction with other fluorescent probes.

Acknowledgments

We thank Dr. Henry A. Lardy for his support and interest during the early stages of this work.

References

Anteunis, M. J. O. (1977) *Bioorg. Chem. 6*, 1–11.

Babcock, D. F., First, N. L., & Lardy, H. A. (1976) *J. Biol. Chem. 251*, 3881–3886.

Babcock, D. F., Stamerjohn, D., & Hutchinson, T. (1978) *J. Exp. Zool. 204*, 391–399.

Babcock, D. F., Chen, J.-L. J., Yip, B. P., & Lardy, H. A. (1979) *J. Biol. Chem. 254*, 8117–8120.

Ben-Hayyim, G., & Krause, G. H. (1980) *Arch. Biochem. Biophys. 202*, 546-557.
Borle, A. B., & Studer, R. (1978) *J. Membr. Biol. 38*, 51-72.
Chandler, D. E., & Williams, J. A. (1978) *J. Cell Biol. 76*, 371-385.
Chaney, M. O., DeMarco, P. V., Jones, N. D., & Occolowitz, J. L. (1974) *J. Am. Chem. Soc. 96*, 1932-1933.
Chen, J.-L. J., Babcock, D. F., & Lardy, H. A. (1978) *Proc. Natl. Acad. Sci. U.S.A. 75*, 2234-2238.
Deber, C. M., & Pfeiffer, D. R. (1976) *Biochemistry 15*, 132-141.
Deber, C. M., Young, M. E. M., & Tom-Kun, J. (1980) *Biochemistry 19*, 6194-6198.
Dordick, R. S., Brierly, G. P., & Garlid, K. D. (1980) *J. Biol. Chem. 255*, 10299-10305.
Ferreira, H. G., & Lew, V. L. (1976) *Nature (London) 259*, 47-49.
Gale, R. M., Higgens, C. E., & Hoehn, M. M. (1976) U.S. Patent 3 960 667.
Kauffman, R. F., Taylor, R. W., & Pfeiffer, D. R. (1980) *J. Biol. Chem. 255*, 2735-2739.
Klausner, R. D., Fishman, M. C., & Karnovsky, M. J. (1979) *Nature (London) 281*, 82-83.
Kretsinger, R. H. (1979) *Adv. Cyclic Nucleotide Res. 11*, 1-26.
Pfeiffer, D. R., & Lardy, H. A. (1976) *Biochemistry 15*, 935-943.
Pfeiffer, D. R., & Deber, C. M. (1979) *FEBS Lett. 105*, 360-364.
Pfeiffer, D. R., Hutson, S. M., Kauffman, R. F., & Lardy, H. A. (1976) *Biochemistry 15*, 2690-2697.
Rasmussen, H., & Goodman, D. B. P. (1977) *Physiol. Rev. 57*, 421-509.
Reed, P. W., & Lardy, H. A. (1972) *J. Biol. Chem. 247*, 6970-6977.
Scarpa, A. (1974) *Biochemistry 13*, 2789-2794.
Smith, G. D., & Duax, W. L. (1976) *J. Am. Chem. Soc. 98*, 1578-1580.
Sokolove, P. M. (1979) *Biochim. Biophys. Acta 545*, 155-164.
Taylor, R. W., Kauffman, R. F., & Pfeiffer, D. R. (1982) in *The Polyether Ionophores* (Westley, J. W., Ed.) Chapter 11, Marcel Dekker (in press).
Westley, J. W. (1976) *J. Antibiot. 29*, 584-586.
Westley, J. W., Oliveto, E. P., Berger, J., Evans, R. H., Jr., Glass, R., Stempel, A., Toome, V., & Williams, T. (1973) *J. Med. Chem. 16*, 397-403.

Interactions of Wild-Type and Mutant M Protein of Vesicular Stomatitis Virus with Viral Nucleocapsid and Envelope in Intact Virions. Evidence from [^{125}I]Iodonaphthyl Azide Labeling and Specific Cross-Linking†

Denise A. Mancarella‡ and John Lenard*

ABSTRACT: Four different temperature-sensitive M protein mutants (tsM) of vesicular stomatitis virus (VSV) were characterized with regard to the association of the mutated M protein either with nucleocapsids or with membranes in the intact virions. Virions were labeled with the photoreactive hydrophobic probe [^{125}I]iodonaphthyl azide (INA) to assess interactions between viral proteins and the lipid envelope. In wild type (wt) virions, the three major structural proteins—G, M, and N—were labeled in the ratio ca. 1.0:0.4:0.2. INA labeled only the membrane-associated peptide of G protein, both in the intact virion and in reconstituted G protein–viral lipid vesicles, demonstrating the specificity of INA for lipid bilayer regions. Labeling of tsM virions with INA resulted in a 2–3-fold greater incorporation into M protein than was found for wt virions, suggesting increased M–membrane associations in the mutant virions. Temperature-stable revertants from tsM possessed wt labeling characteristics. Interaction of the M protein with nucleocapsids was assessed from the abundance of disulfide-linked M–N complexes found after disruption of the virions by sodium dodecyl sulfate solution under nonreducing conditions. The abundance of such complexes was 30–80% less from tsM virions than from wt virions, suggesting decreased M–nucleocapsid interactions in tsM virions. Temperature-stable revertants from tsM resembled wt in the abundance of M–N complex formed. We conclude that the mutations alter M protein in such a way as simultaneously to increase its association with membrane and to decrease its affinity for nucleocapsids in the intact virion.

The vesicular stomatitis virus (VSV)[1] matrix (M) protein, a nonglycosylated polypeptide of M_r 27 000, is one of the three major structural proteins of the virion (Bishop & Smith, 1978). Recent experiments utilizing VSV temperature-sensitive (ts) mutants and viral pseudotypes have shown that M protein is essential for the budding of virions or virus-like particles from the plasma membrane of an infected cell (Schnitzer et al., 1979; Schnitzer & Lodish, 1979; Weiss & Bennett, 1980). Specific functional interactions between M protein and viral nucleocapsid on the one hand and between M protein and membrane containing the viral glycoprotein (G) on the other

† From the Department of Physiology and Biophysics, College of Medicine and Dentistry of New Jersey, Rutgers Medical School, Piscataway, New Jersey 08854. *Received May 5, 1981.* Supported by Grant No. AI 13002 from the National Institutes of Health and Grant No. 1-683 from the National Foundation—March of Dimes. The INA labeling results reported here were presented in preliminary form at the 71st Annual Meeting of the American Society of Biological Chemists, New Orleans, LA, June 1980.
‡ Supported by National Institutes of Health Training Grant Ca 09069.

[1] Abbreviations used: VSV, vesicular stomatitis virus; wt, wild-type VSV; wtO, wild-type VSV, Orsay variant; wtG, wild-type VSV, Glasgow variant; ts, temperature sensitive; tsM, temperature-sensitive mutant of complementation group III; $NaDodSO_4$, sodium dodecyl sulfate; [^{125}I]-INA, 5-iodonaphthyl 1-azide containing ^{125}I.

0006-2960/81/0420-6872$01.25/0